Exploring of hypoglycemic mechanism of a Chinese Medicine Xiao-Ke-An based on target dipeptidyl peptidase-4□a molecular docking and molecular dynamics study

Yong-Lin WANG (✉ 18339913895@163.com)
Henan University of Chinese Medicine
Yan ZHUANG
Henan University of Chinese Medicine
Yan TONG
Henan University of Chinese Medicine
Yuan-Fang KONG
Henan University of Chinese Medicine
Yu-Long HU
Henan University of Chinese Medicine
Jie-Ming LI
Henan University of Chinese Medicine
Shao-Pei WANG
Henan University of Chinese Medicine
Chun-Hong DONG
Henan University of Chinese Medicine https://orcid.org/0000-0002-3251-8926
Xiao-Fei LI
Henan University of Chinese Medicine

Research Article

Keywords: DPP-□, Xiaokean, Docking, Molecular dynamics, MM/PBSA, Binding free energy

Posted Date: March 16th, 2021

DOI: https://doi.org/10.21203/rs.3.rs-325933/v1

Exploring of hypoglycemic mechanism of a Chinese Medicine Xiao-Ke-An based on target dipeptidyl peptidase-4：a molecular docking and molecular dynamics study

WANG Yong-Lin, ZHUANG Yan, TONG Yan, KONG Yuan-Fang, HU Yu-Long, LI Jie-Ming, WANG Shao-Pei , DONG Chun-Hong*, LI Xiao-Fei*

(Henan University of Chinese medicine, Zhengzhou 450046 China)

Abstract: Xiao-Ke-An, a traditional Chinese medicine formula against diabetes in China, is reported inhibitory activity on Dipeptidyl peptidase-4 (DPP-4). However, its molecular mechanism is still unclear due to the complexity of its components. In this study, a combination of molecular docking, molecular dynamics (MD) and molecular mechanics/Poisson Boltzmann surface area (MM-PBSA) method was conducted. The results show that multiple components of Xiao-Ke-An can take effect on DPP-4 together, which could be the part of the hypoglycemic mechanism of Xiao-Ke-An. Of the eight selected compounds, MOL003714 shows the highest activity for inhibiting DPP-4 with the binding free energy of -44.14 kcal·mol^{-1} via binding to the S_2 and S'_1 subsites of DPP-4, which could be a potent inhibitor for DPP-4. This study provided theoretical basis for the discovery and modification of natural DPP-4 inhibitors and the deeply insight into Xiao-Ke-An.

Keywords: DPP-Ⅳ; Xiaokean; Docking; Molecular dynamics; MM/PBSA; Binding free energy

1. Introduction

Glucagon-like peptidase-1 (GLP-1) is a 30-amino-acid incretin secreted by L-cells in the lower digestive tract. It can promote the transcription of insulin genes and proliferation of β-cell and increase the biosynthesis and secretion of insulin by acting on pancreatic β-cells in a glucose-dependent manner, at the same time, it can inhibit the secretion of glucagon of α-cell. Thereby, GLP-1 plays an important role in maintaining blood glucose level. Dipeptidyl peptidase-4 (DPP-4) is a kind of serine proteinase mainly expressed in small intestine, liver, kidney, pancreas and spleen. In vivo, it can resolve GLP-1, resulting in the decreasing of insulin

* Corresponding author e-mail: chunhong_dong@hactcm.edu.cn; * Corresponding author e-mail: arphylee@126.com

secretion and the occurrence of diabetes[1-3]. DPP-4 has become a hot target in the development of hypoglycemic drugs recently. Its active pocket is composed of five subsites, S_1, S_2, S'_1, S'_2 and S_2-extensive subsites (Figure 1). It recognizes N-terminal of GLP-1 from amino terminus preferentially having proline or alanine residues at penultimate position through the S_2 subsite, then the dipeptide was cleaved by Ser630 of the S_1 subsite[4]. Based on these subsites, especially the S_1 and S_2 subsites, several DPP-4 inhibitors have been successfully developed and available on market, such as sitagliptin, linagliptin, vildagliptin, saxagliptin, etc[3, 5]. These drugs have different binding modes in DPP-4 active pocket[6-8]. Vildagliptin and saxagliptin were designed as peptidemimetics inhibitors, whose cyanopyrrolidine moieties bind to the S_1 subsite and form a covalent bond between nitrile group and Ser630. The hydroxy adamantyl groups bind to the S_2 subsite, and the nitrogen atom of amino group forms a salt bridge that connected Glu205 and Glu206[9, 10]. In addition to the S_1 and S_2 subsites, alogliptin and linagliptin bind to the S'_1 subsite, forming π-π interaction between Tyr547 and their uracil rings, and the phenyl of the quinazoline substituent in linagliptin forms a π-π interaction with Trp629 in the S'_2 subsite[6,11]. The triazolopyrazine moiety of sitagliptin, 1-phenylpyrazol and piperazine moiety of teneligliptin bind to the S_2-extensive subsite (Arg358, Phe357) mainly by forming hydrogen bond or π-π interaction with Phe357[12, 13]. The less cardioprotective effect of DPP-4 inhibitors and their low risk of causing hypoglycaemia makes them become widely used as second-line agents[5, 14, 15] . Other excellent natural DPP-4 inhibitors, such as chrysin[16], galangin[17], plectranthoic acid[18], iso-daphnetin[19, 20], polyphenols, flavonoids[21] and cyanidin 3,5-diglucoside[22] are now in the pre-clinical phases. In addtion, a variety of other plant-derived compounds including alkaloids, terpenoids, steroids, phenols, peptides, flavonoids, resveratrol, cyanidins and triterpenes have also been reported have activities for DPP-4[23-25].

Xiao-Ke-An, a traditional Chinese medicine formula composed of *Rehmanniae Radix Praeparata*, *Anemarrhenae Rhizoma*, *Coptidis Rhizoma, Lycii Cortex*, *Lycii Fructus, Polygonati Odorati Rhizoma*, *Panax Ginseng C. A. Mey.* and *Radix Salviae*[26], is widely used for the treatment of type II diabetes mellitus in China with low cost and minimal side effect[27]. Wu Xue and his colleagues verified that some components in Xiao-Ke-An have DPP-4 activity, and screened out some salvianolic acids and saponins with strong inhibitory effect on DPP-4[28]. The subsequent studies proved that many components in Xiao-Ke-An could activate AKT/GSK-3β

pathway by inhibiting DPP-4 and improving glucose and lipid metabolism[27]. However, systematical screening of all possible components with DPP-4 activity in Xiao-Ke-An has not been studied and their binding modes between the active components and DPP-4 are still unclear.

In this study, a database containing 819 components of Xiao-Ke-An for virtual screening was obtained by molecular docking method, and the binding modes between active components and DPP-4 were furtherly explored through molecular dynamics simulation. It was expected the results could explain the hypoglycemic molecular mechanism of Xiao-Ke-An and promote the discovery of new DPP-4 inhibitors and the deeply insight into Xiao-Ke-An.

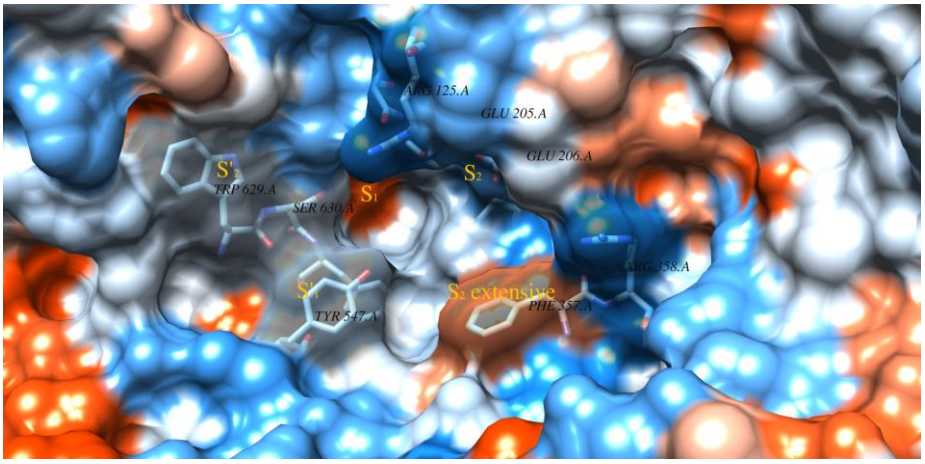

Figure 1 The distribution of each subsite of DPP-4

2. Method

2.1 Molecular docking

2.1.1 Preparation of components database of Xiao-Ke-An

The 3D structure of the components of Xiao-Ke-An were downloaded from the traditional Chinese medicine systems pharmacology database and analysis platform(TCMSP, https://tcmspw.com/tcmsp.php)[29], and optimized by using MMF94 force.

2.1.2 Preparation of DPP-4

The crystal structure of DPP-4 was derived from RCSB protein data bank database(PDB ID: 3VJK)[30]. 3VJK is composed of DPP-4 and its ligand, an inhibitor named teneligliptin. It has four same chains, A, B, C and D, and the active site is in each chain, so only chain A was used for molecular docking and the following molecular dynamics simulation in this study. Prior to the

molecular docking, crystal water molecules and the ligand were removed, and hydrogen atoms were added with Autodock Tools 1.5.6 package[31].

2.1.3 Molecular docking

Autodock Vina 1.1.2[32] was used for molecular docking. All small molecules were kept flexible and the receptor DPP-4 was kept rigid. The exhaustiveness parameter was set to 10, the center coordinates of the box was (48.68, 62.15, 32.28), the number of grid points of the box was (30, 26, 30), the grid spacing was set to 1 Å, and the number of generated modes was set to 10. All other parameters were set as default values.

2.2 Molecular dynamics simulation

Molecular dynamics simulations were conducted with Amber18 package[33,34]. The optimal conformation of each docking result was used for the initial structure of dynamic simulation. Prior to the dynamic simulation, Gaussian 09[35] was used to construct small molecule force field under the level of HF/6-31G*, and RESP (Restrained ElectroStatic Potential) was used to generate atom charge. Topology and coordinate files were generated through *tleap*. All parameters were established under ff14SB and GAFF force field[36]. Each system was solvated in an octahedral water box with TIP3P water model and periodic boundary of 10 Å. Na^+ was added as the counter-ion to neutralize the system.

The energy minimization was divided into three steps: Firstly, energy minimization with the complex constrained. The maximum number of cycles was set to 4000 steps. Steepest descent method was used for the first 2000 steps, and the conjugate gradient method for the next 2000 steps. Secondly, energy minimization with the protein skeleton constrained. The maximum number of cycles was 5000 with the steepest descent method for the first 2500 steps and the conjugate gradient method for the 2501-5000 steps. Finally, energy minimization without any constraints. The maximum number of cycles was 10000. The steepest descent method was used in the first 5000 steps, and the conjugate gradient method was used in 5001 to 10000 steps.

The system was firstly heated for 40 ps from 0 K to 300 K in a NVT ensemble by Berendsen control method, then equilibrated at 300 K for another 20 ps. 100 ns production simulation was

finally performed at constant pressure and constant temperature under periodic boundary conditions by Berendsen control method.

2.3 Binding free energy calculation

The final 5 ns stable MD trajectory was selected to calculate the binding free energy with MM-PBSA[37] method in Amber18. The binding free energy ($\Delta G_{binding}$)is calculated by the following equations[38]:

$$\Delta G_{binding} = \Delta G_{complex} - [\Delta G_{protein} + \Delta G_{ligand}] \quad (1)$$

$$\Delta G_{binding} = \Delta E_{gas} + \Delta G_{sol} - T\Delta S \quad (2)$$

$$\Delta E_{gas} = \Delta E_{ele} + \Delta G_{vdW} \quad (3)$$

$$\Delta G_{sol} = \Delta G_{polar} + \Delta G_{nopolar} \quad (4)$$

$\Delta G_{complex}$, $\Delta G_{protein}$ and ΔG_{ligand} are the free energies of complex, protein and ligand respectively. ΔE_{gas} and ΔG_{sol} are the gas phase interaction energy and the solvation free energy respectively; ΔE_{ele} and ΔG_{vdW} are the electrostatic energy and van der Waals energy respectively; ΔG_{polar} and $\Delta G_{nopolar}$ are the polar contribution and van der nopolar contribution respectively. The entropy contribution (ΔS) was ignored in this study, considering that the computation of entropy contribution by normal mode analysis (NMA) approach is computationally expensive and tends to have a large error that introduces significant uncertainty in the result[39].

3. Results and discussion

3.1 Molecular Docking

45 compounds with higher docking score than tenegliptin (ΔG_{score}= -8.4 kcal·mol^{-1}) were initially screened from molecular docking and furtherly screened according to drug-likeness (DL) parameter (DL>0.18) in TCMSP database. 17 compounds were finally obtained. These compounds were divided into three groups, phenols group, steroids group and other group based on their structure characteristic. Finally, eight compounds with the lowest binding energies of each sub-group were selected for the following research, which are shown in Table 1. Phenols group

includes dimetbyl lithosper-mate B, jionoside A and physcion-8-O-beta-D-gentiobioside; Steroidal group includes polygosides A and ginsenoside Rg5, other group contains three compounds, neoprzewaquinone A, dauricine and limonin.

Table 1 Docking results of 8 compounds with DPP-4

Group name	Origin	Compounds (sub-group name)	Structure	Binding energy (kcal·mol^{-1})
Phenols	*Radix Salviae*	MOL007103 （Dimetbyl Lithosper-mate B）	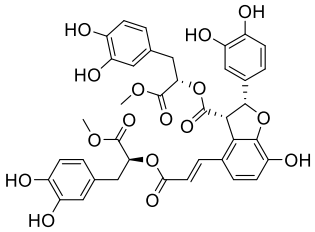	-10.1
	Rehmanniae Radix Praeparata	MOL003714 （Jionoside A）	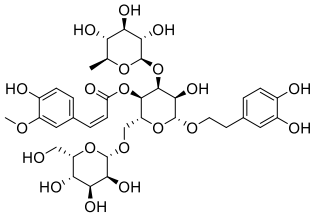	-10.1
	Lycii Fructus	MOL009665 （Physcion-8-O-beta-D-gentio bioside）	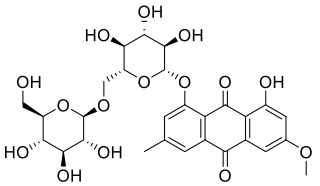	-9.6
Steroids	*Polygonati Odorati Rhizoma*	MOL010404 （Polygosides A）	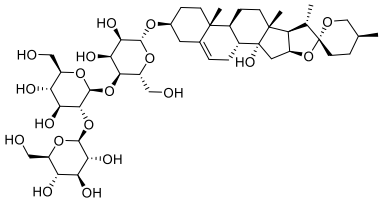	-10.4
	Panax Ginseng C. A. Mey.	MOL005400 （Ginsenoside Rg5）	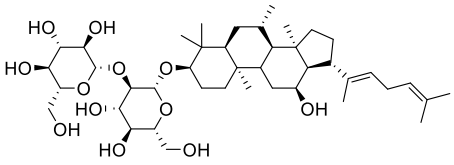	-9.9

	Radix Salviae	MOL007062 （Neoprzewaquinone A）	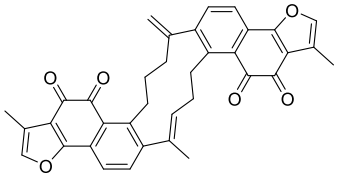	-11.0
Other	*Panax Ginseng C. A. Mey.*	MOL001965 （Dauricine）	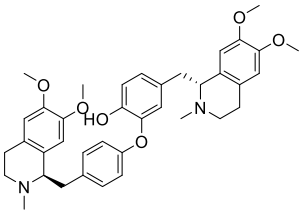	-10.1
	Coptidis Rhizoma	MOL003959 （Limonin）	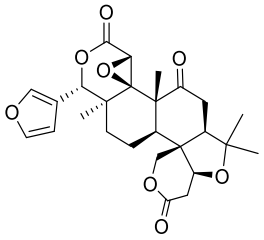	-9.6

3.2 MD simulations

3.2.1 RMSD analysis

The RMSD results of the eight complexes were shown in Figure 2. RMSD of MOL007103 has a large deviation at about 9 ns when the ligand adjusts itself to a new position, then keeps stable at about 3Å. But, at 55 ns the RMSD of MOL007103 began to fluctuate. (Figure 2a). The superposition of initial conformation, conformations at 50 ns and 100 ns of DPP-4 complex shows that the conformation at 100 ns deviates from that at 50 ns (Figure 3a), suggesting that the ligand didn't reach a stable state after the dynamics simulations. The RMSD of MOL003714 keeps stable at about 2.4 Å and the RMSD of the complex keeps stable at about 3.0 Å shortly after the MD simulation (Figure 2b). The coincidence of the conformations at 10 ns and 100 ns also indicates that the complex reaches a stable state(Figure 3b). For MOL009665, its RMSD keeps stable at 1.9 Å during the 88 ns simulation. But, after 88 ns, the RMSD jumps to about 4 Å gradually (Figure 2c). The conformations at 50 ns and 100 ns do not keep a constant orientation in the active site of DPP-4 (Figure 3c). For MOL010404 and its complex with DPP-4, their RMSDs keep nearly constant after 3 ns (Figure 2d). The similar orientation of the conformations at 10 ns and 100 ns also prove the stability of the complex (Figure 3d). RMSD of MOL005400 increases at about 3 ns,

then reaches stable at about 3 Å (Figure 2e). The conformation of the complex keeps almost constant (Figure 3e). The RMSD of MOL001965 stabilizes at 3.5 Å after an adjustment compared with the initial conformation at about 2 ns (Figure 2g, Figure 3g). In the eight systems, MOL007062 and MOL003959 are the most stable, which could be seen from both of their RMSDs and the superposition results (Figure 2f, 3f, 2h, 3h).

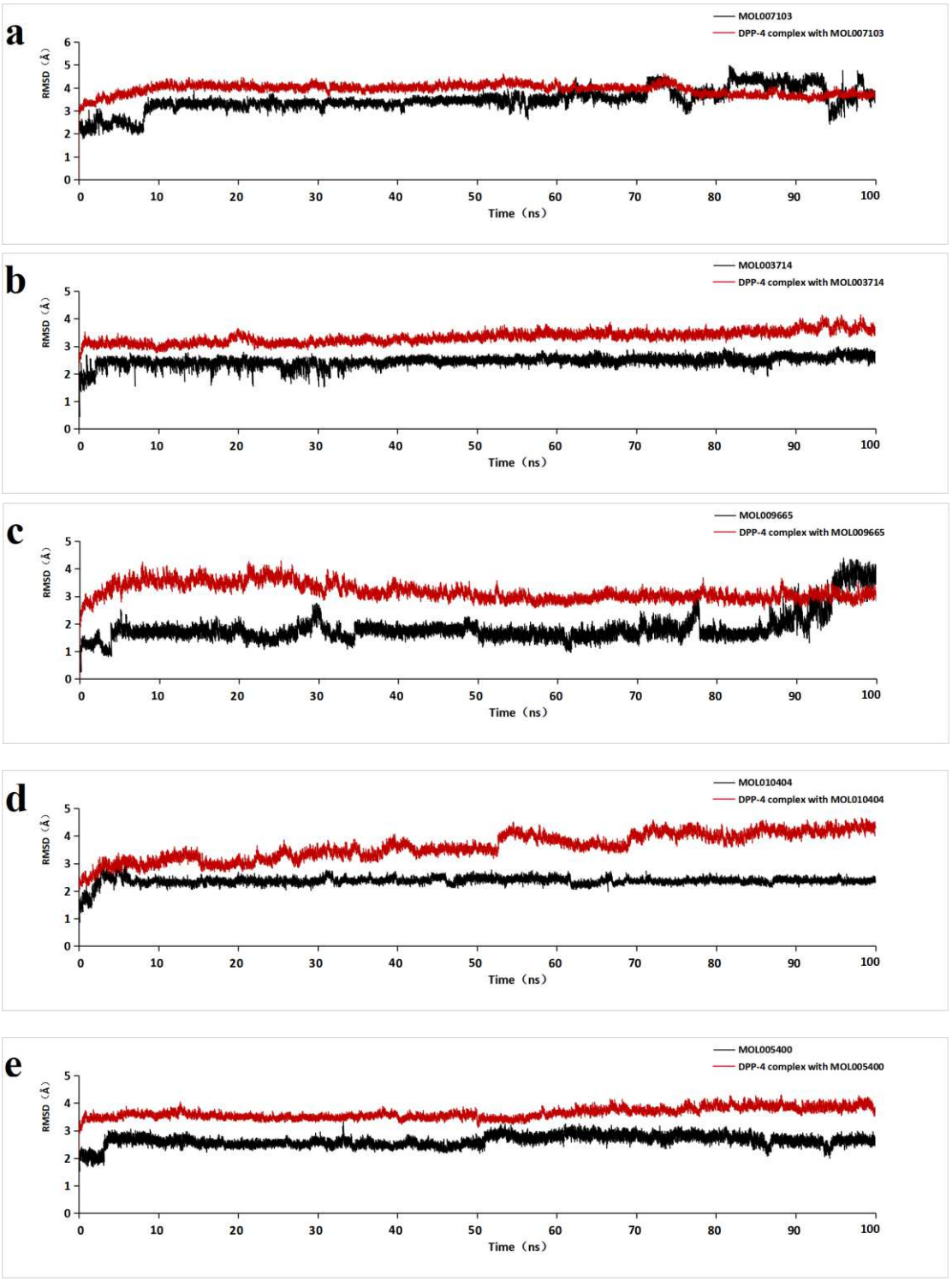

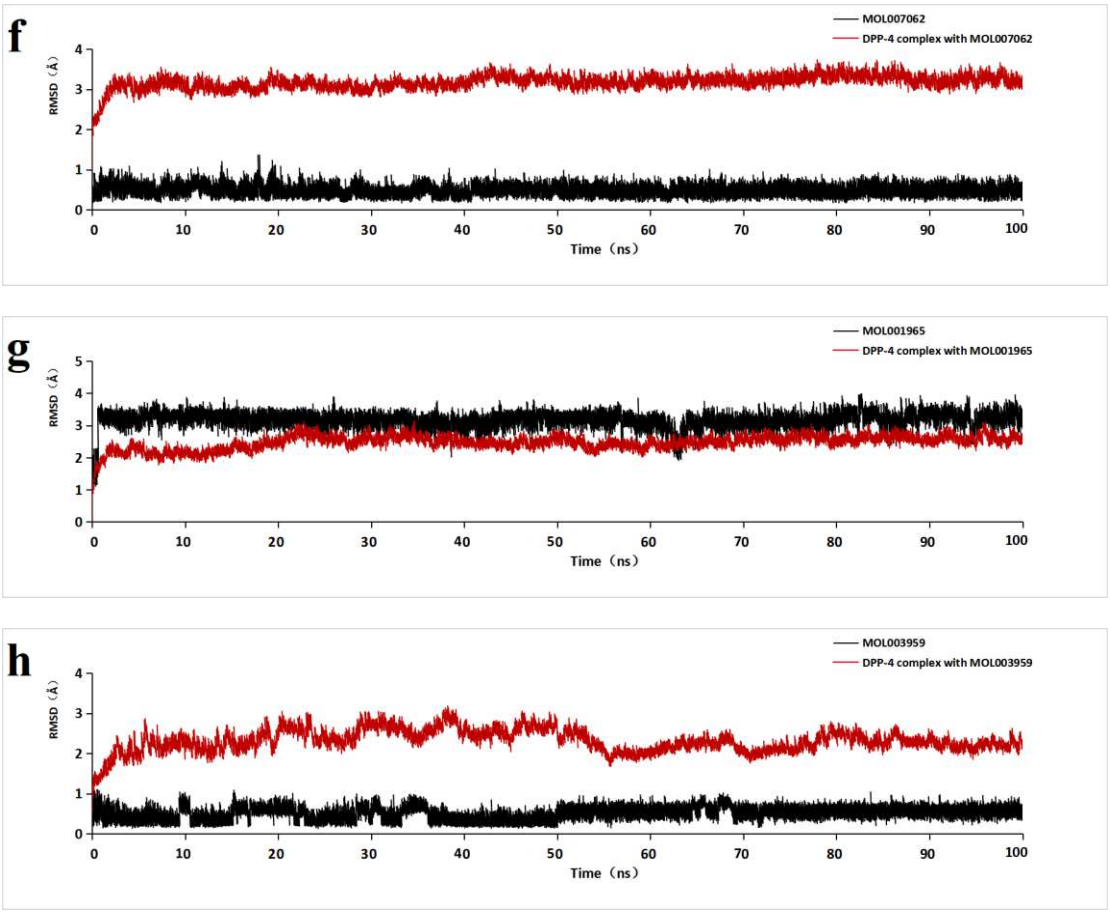

Figure 2. RMSD plots of DPP-4 in complex with MOL007103 (a), MOL003714 (b), MOL009665 (c), MOL010404 (d), MOL005400 (e), MOL007062 (f), MOL001965 (g) and MOL003959 (h).

Totally, RMSD analysis indicates that except MOL007103 and MOL009665, other six compounds successfully bind to the active pocket of DPP-4 and reach their equilibrium states in 100 ns simulation process.

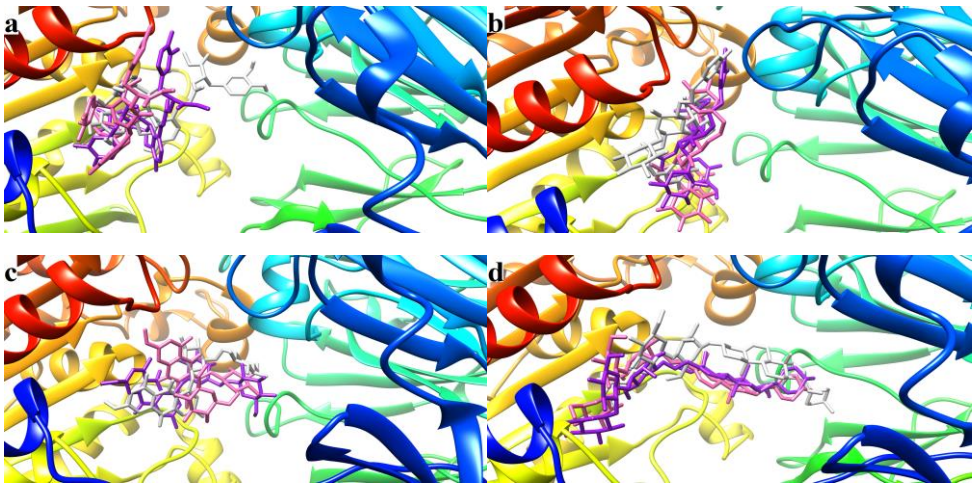

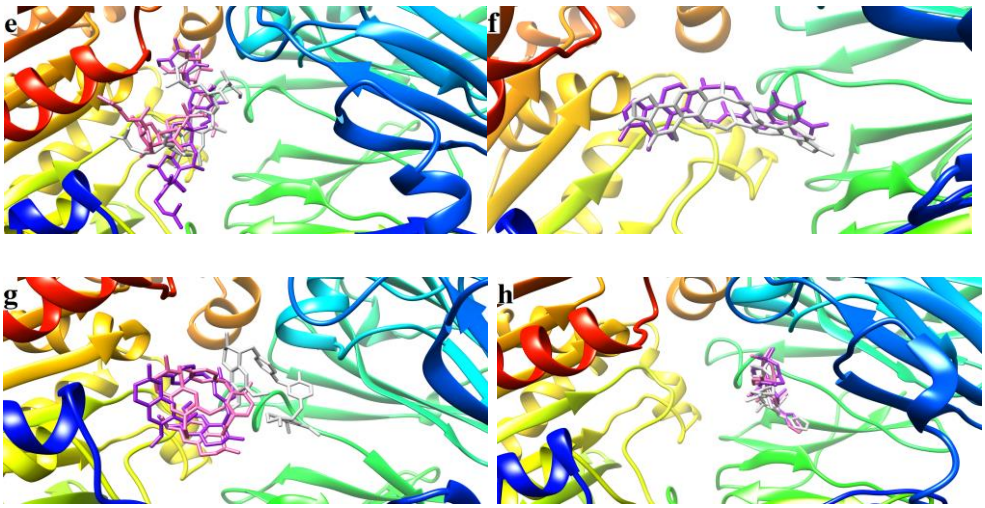

Figure 3. Superposition of the eight compounds in the dynamics simulation process. The ribbon model represents DPP-4. The stick model represents the eight compounds, gray stick represents the initial conformation. In (a), purple and pink sticks represent the conformations of MOL007103 at 50 ns and 100 ns, respectively; In (b), purple and pink sticks represent the conformations of MOL003714 at 10 ns and 100 ns, respectively; In (c), purple and pink sticks represent the conformations of MOL009665 at 50 and 100 ns, respectively; In (d), purple and pink sticks represent the conformations of MOL010404 at 10 ns and 100 ns, respectively; In (e), purple and pink sticks represent the conformations of MOL005400 at 5 ns and 100 ns, respectively; In (f), pink sticks represent the conformation of MOL007062 at 100 ns; In (g), purple and pink sticks represent the conformations of MOL001965 at 2 ns and 100 ns, respectively; In (h), purple, pink and orange sticks represent the conformations of MOL003959 at 50 ns and 100 ns, respectively.

3.2.2 Binding free energy

The binding free energies calculation for 2500 snapshots of the eight complexes were performed from the final 5 ns simulation by MM-PBSA method, and the results were shown in Table 2.

Table 2 Binding free energies of eight compounds with DPP-4 (kcal·mol^{-1})

Compound	Van der Waals	Electrostatic force	Polar solvation	Nonpolar solvation	$\Delta G_{binding}$
MOL007103	-36.81	-40.55	59.08	-4.28	-22.56
MOL003714	-52.60	-95.15	110.00	-6.39	-44.14
MOL009665	-31.96	-53.94	63.71	-3.92	-26.11

MOL010404	-54.54	-86.58	104.91	-6.42	-42.63
MOL005400	-55.00	-65.71	101.74	-6.72	-25.69
MOL007062	-41.70	-14.18	37.74	-4.00	-22.14
MOL001965	-43.19	-5.53	32.17	-4.23	-20.78
MOL003959	-46.01	-24.02	49.04	-3.58	-24.57

As shown in Table 2, the main contributions for binding free energies are van der Waals force and electrostatic force, while polar solvation energy is not conducive to the binding of the ligands with DPP-4. The binding free energies of the eight complexes are ranged from -44.14 to -20.78 kcal·mol^{-1}, suggesting the binding of each compound with DPP-4 is a thermodynamically favorable process. MOL003714 has the lowest binding free energy and electrostatic force, which are -44.14 kcal·mol^{-1} and -95.15 kcal·mol^{-1}. Except for MOL007103, MOL007062, MOL001965 and MOL003959 have higher binding free energies than the other compounds, which are -22.14 kcal·mol^{-1}, -20.78 kcal·mol^{-1} and -24.57 kcal·mol^{-1} respectively. By comparing the structures of each compound, it is found that the more hydroxyl groups in the molecule form hydrogen bonds with the relevant residues, especially Arg125, Glu205 and Glu206, the lower binding free energy and the larger electrostatic interaction contribute (Figure 4). However, MOL007103 has deviated from the active site, so the hydroxyl groups of it didn't form hydrogen bonds with Glu205 and Glu206.

3.2.3 Decomposition free energy and binding mode analysis

To explore the interaction modes of each molecule that binds to DPP-4, decomposition free energy of the selected residues were calculated by using MM-PBSA method. The decomposition free energy of the residues are shown in Figure 5.

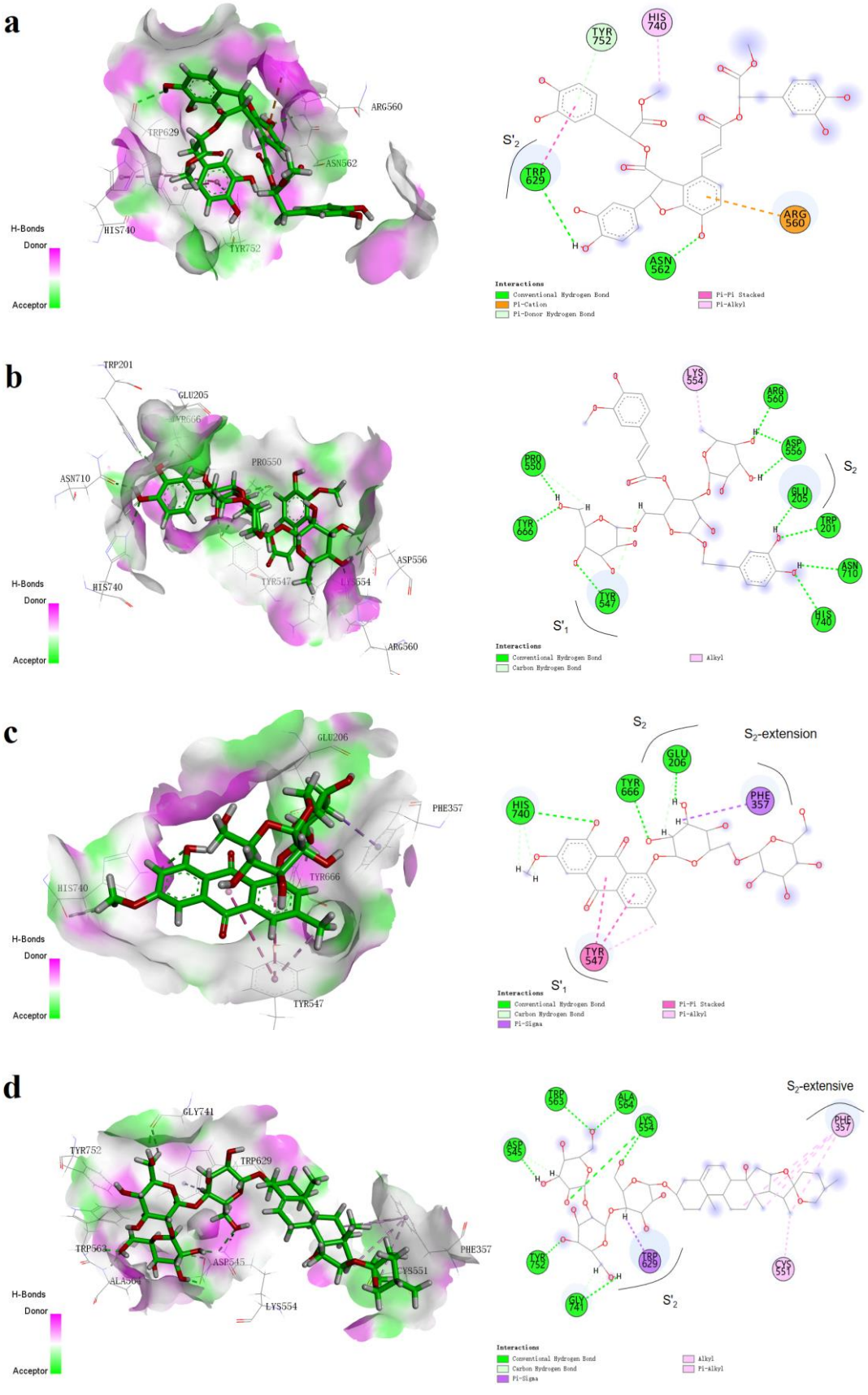
a
ARG560
TRP629
ASN562
HIS740
TYR752
H-Bonds
Donor
Acceptor
HIS 740
TYR 752
S'2
TRP 629
ARG 560
ASN 562
Interactions
Conventional Hydrogen Bond
Pi-Cation
Pi-Donor Hydrogen Bond
Pi-Pi Stacked
Pi-Alkyl
b
TRP201
GLU205
ASN710
PRO550
ASP556
TYR547
LYS554
ARG560
HIS740
H-Bonds
Donor
Acceptor
LYS 554
ARG 560
ASP 556
PRO 550
S2
GLU 205
TYR 666
TRP 201
ASN 710
TYR 547
HIS 740
S'1
Interactions
Conventional Hydrogen Bond
Carbon Hydrogen Bond
Alkyl
c
GLU206
PHE357
TYR666
HIS740
TYR547
H-Bonds
Donor
Acceptor
S2
S2-extension
GLU 206
TYR 666
PHE 357
HIS 740
TYR 547
S'1
Interactions
Conventional Hydrogen Bond
Carbon Hydrogen Bond
Pi-Sigma
Pi-Pi Stacked
Pi-Alkyl
d
GLY741
TYR752
TRP629
TRP563
ASP545
ALA564
LYS554
PHE357
LYS551
H-Bonds
Donor
Acceptor
S2-extensive
TRP 563
ALA 564
LYS 554
PHE 357
ASP 545
TYR 752
TRP 629
CYS 551
GLY 741
S'2
Interactions
Conventional Hydrogen Bond
Carbon Hydrogen Bond
Pi-Sigma
Alkyl
Pi-Alkyl

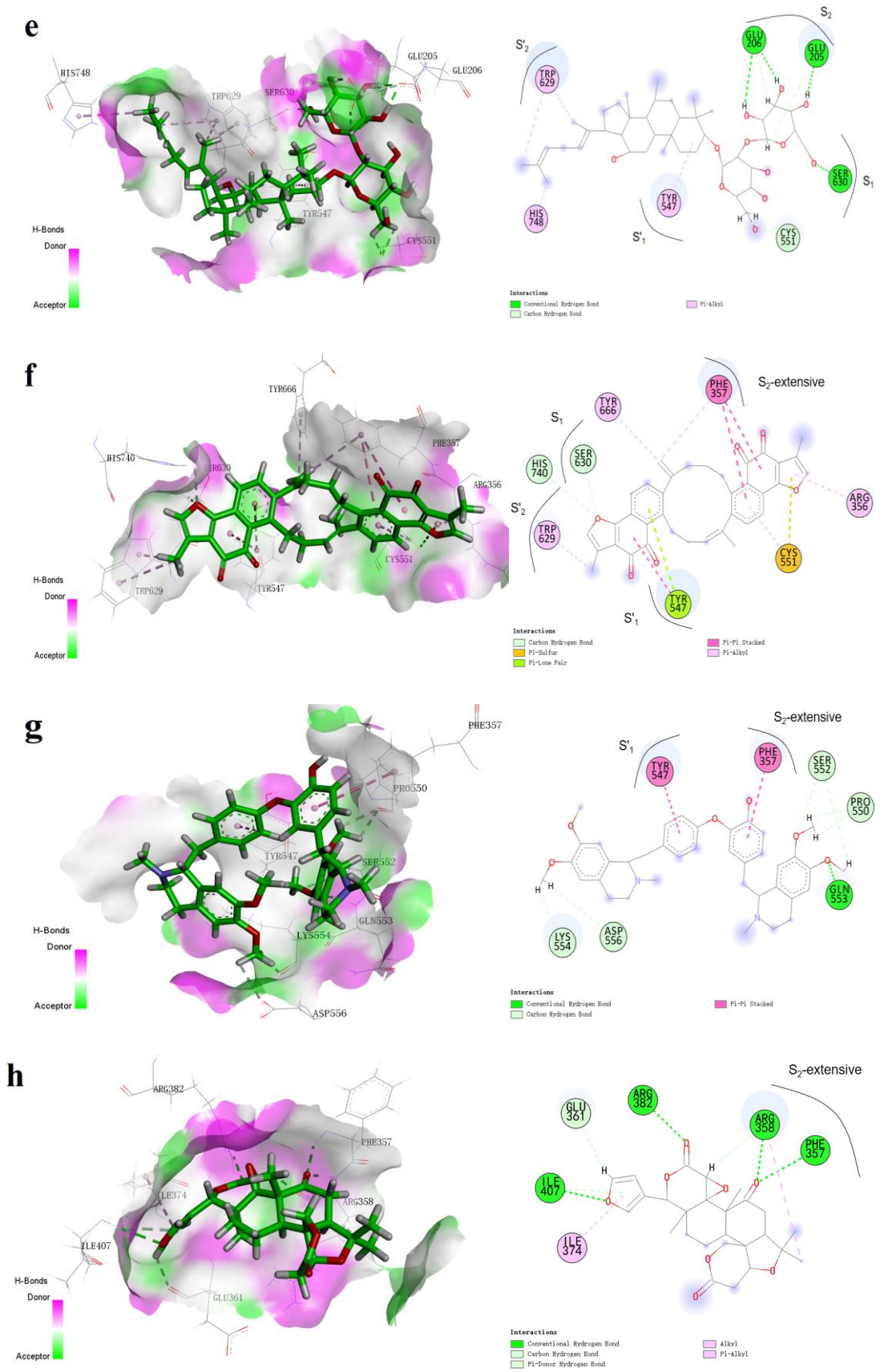

Figure 4 Binding modes and interaction diagrams of MOL007103 (a), MOL003714 (b), MOL009665 (c), MOL010404 (d), MOL005400 (e), MOL007062 (f), MOL001965 (g) and MOL003959 (h) with DPP-4.

MOL007103, a salvianolic acid compound, contains four phenolic rings and seven phenolic hydroxyl groups. After reaching the stable state, Trp629 forms Pi-Pi interaction with nearby benzene ring and a O-H···O hydrogen bonds with hydroxyl group on another benzene ring; Tyr547 maybe form van der Waals force with MOL007103. The binding free energy of them are 2.32 kcal·mol^{-1}and 1.35 kcal·mol^{-1}, respectively. However, it can be seen from Figure 2a, Figure3a that MOL007103 did not reach a stable state in the process of dynamic simulation, and deviated from the S_1 and S_2 subsites gradually. So, MOL007103 does not bind to DPP-4 stably (Figure 4a, Figure 5a).

MOL003714 is a caffeic glycoside compound. When reaching the stable state, the oxygen atom of -COO$^-$ of Glu205 in the S_2 subsite forms an O-H···O hydrogen bonds with hydroxyl group on the phenol ring. Meanwhile, Tyr547 in the S'_1 subsite forms an O-H···O hydrogen bond with its adjacent sugar ring, the binding free energies of the residues are -0.091 kcal·mol^{-1} and -3.93 kcal·mol^{-1}. Except the residues formed hydrogen bonds interaction with MOL003714, the residues , such as Arg125, Phe357, Trp629 and Tyr631, may also contribute to the binding free energy.via van der Waals force. The binding free energies of the five residues are -2.10 kcal·mol^{-1}, -1.18 kcal·mol^{-1},-1.0 kcal·mol^{-1} and -0.87 kcal·mol^{-1} respectively. Besides, Pro550, Asp556 and Tyr666 also have significant contribution to binding free energy. Thus MOL003714 binds to the S_2, S_1' subsites of DPP-4 stably mainly by hydrogen bonds interaction with Glu205 and Tyr547 and other van der Waals force interactions between MOL003714 and DPP-4, which result in the lowest binding free energy with DPP-4 (Figure 4b, Figure 5b).

MOL009665 belongs to anthraquinone glycoside, which contains a conjugated anthraquinone moiety and two sugar rings. Two of oxygen atoms on -COO$^-$ of Glu206 form a C-H···O hydrogen bond with alkyl hydrogen and an O-H···O hydrogen bond with hydroxyl hydrogen on the sugar ring. Phe357 in the S_2-extensive subsite forms Pi-Sigma interaction with hydrogen atom on the same sugar ring; Tyr547 forms Pi-Pi and Pi-alkyl interactions with anthraquinone moiety, and the binding free energy of the three residues are -2.79 kcal·mol^{-1}, -1.91 kcal·mol^{-1} and -1.34 kcal·mol^{-1}, respectively. However, the RMSD of MOL009665 fluctuates at about 88 ns (Figure 2c), and the terminal sugar ring deviates from the S_1 and S_2 subsites gradually (Figure 3c). So it is indicated that MOL009665 could not bind to DPP-4 stably (Figure 4c, Figure 5c).

MOL010404 belongs to steroidal saponins. It mainly acts on the S'_2 and S_2-extensive subsites

of DPP-4. Phe357 in the S_2-extensive subsite forms Pi-alkyl and Alkyl interactions with tetrahydrofuran ring, etrahydropyrane ring and methyl carbon atom on them; Trp629 in the S'_2 subsite forms Pi-sigma interaction with hydrogen atom on the sugar ring. The binding free energy of them are -1.19 kcal·mol^{-1} and -3.69 kcal·mol^{-1}, respectively. Additionally, Asp545 contributes -5.23 kcal·mol^{-1} to the binding free energy by an O-H···O hydrogen bond and a C-H···O hydrogen bond as a hydrogen bonding acceptor between Asp545 and the hydroxyl group on the terminal sugar ring of MOL010404 (Figure 4d, Figure 5d).

Compared with MOL010404, MOL005400 also belongs to steroidal saponins with only two sugar rings and without C=C and 1,6-dioxaspiro[4.5]decane in its scaffold. At the stable state, two of oxygen atoms on -COO$^-$ of Glu205 forms a C-H···O hydrogen bonds with alkyl hydrogen and an O-H···O hydrogen bond with hydroxyl hydrogen on the terminal sugar ring; One of oxygen atoms on -COO$^-$ of Glu206 forms two O-H···O hydrogen bonds with hydroxyl hydrogens and a C-H···O hydrogen bond with alkyl hydrogen on the terminal sugar ring; Besides, Tyr547 forms Pi-alkyl with alkane ring, Trp629 forms two Pi-alkyl interactions with alkyl carbon atoms nearby it, and Ser630 forms a O-H···O hydrogen bond with hydroxyl hydrogens on the terminal sugar ring of MOL010404; While, Phe357 and Arg125 maybe form van der Waals force with the sugar ring. The binding free energy of them are -1.56 kcal mol^{-1}, -2.61 kcal·mol^{-1}, -0.83 kcal·mol^{-1}, -2.4 kcal·mol^{-1}, -1.90 kcal·mol^{-1}, -3.10 kcal·mol^{-1} and -1.09 kcal·mol^{-1}, respectively. Other residues, such as Tyr666 and Arg669, maybe also form van der Waals force with MOL005400. MOL005400 binds mainly to the S_1, S_2, S'_1 and S'_2 subsites, which is different to its analogue MOL010404 whose main acting subsites are the S'_2 and S_2-extensive subsites (Figure 4e**,** Figure 5e).

MOL007062 is a quinone compound, which contains a large conjugated structure containing aromatic rings. Phe357 forms Pi-Pi interactions with naphtho[1,2-b]furan-4,5-dione ring and Pi-alkyl with vinyl carbon atoms on 12-membered ring; Try547 forms Pi-Pi and Pi-Lone Pair interactions with naphtho[1,2-b]furan-4,5-dione ring; Trp629 forms Pi-Alkyl with the methyl carbon atoms; Ser630 forms a C-H···O hydrogen bond with oxygen atom on naphtho[1,2-b]furan-4,5-dione ring. The binding free energy of them are -2.09 kcal·mol^{-1}, -1.64 kcal·mol^{-1}, -0.79 kcal·mol^{-1}, -0.16 kcal·mol^{-1}, respectively. The binding site is mainly in the S_1, S'_1, S'_2 and S_2-extensive subsites (Figure 4f, Figure 5f).

MOL001965 is a tetra-hydroquinoline alkaloid. After reaching a stable state, Phe357 forms Pi-Pi stacked interaction with the benzene ring; Tyr547 forms Pi-Pi stacked interaction with another benzene ring; While, Arg358 and Trp629 maybe form van der Waals force with MOL001965. The binding free energy of the four residues are -0.46 kcal·mol^{-1}, -1.62 kcal·mol^{-1}, -0.43 kcal·mol^{-1}and -0.87 kcal·mol^{-1}, respectively. It is indicated that MOL001965 mainly binds to the S'$_1$ and S$_2$-extensive subsites (Figure 4g, Figure 5g).

MOL003959, a terpenoid compound, is composed of alkylene oxide and cycloalkanone. In S$_2$-extensive subsite, Phe357 forms N-H···O hydrogen bond interaction with carbonyl oxygen on cyclohexanone, and Arg358 also forms N-H···O hydrogen bond interaction with the same carbonyl oxygen, an alkyl interaction with methyl group on tetrahydrofuran ring and a C-H···O hydrogen bond interaction with hydrogen atom on ethylene oxide, the binding free energy of which are -1.33 kcal·mol^{-1} and -1.44 kcal·mol^{-1}, respectively. (Figure 4h, Figure 5h).

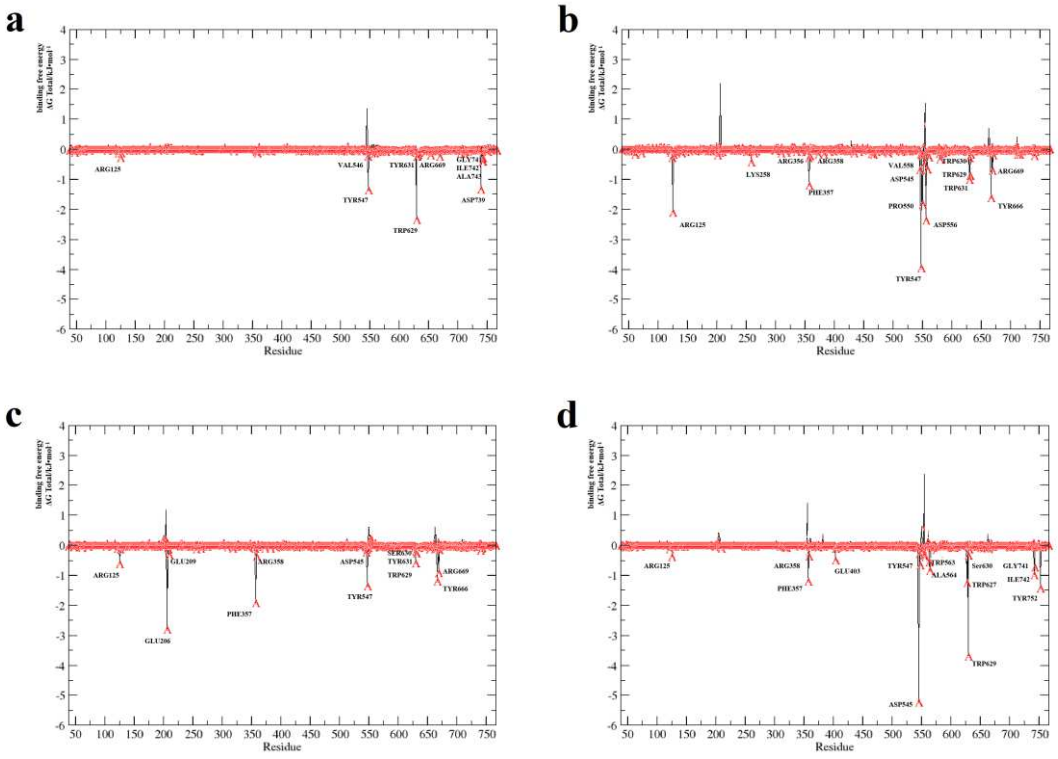

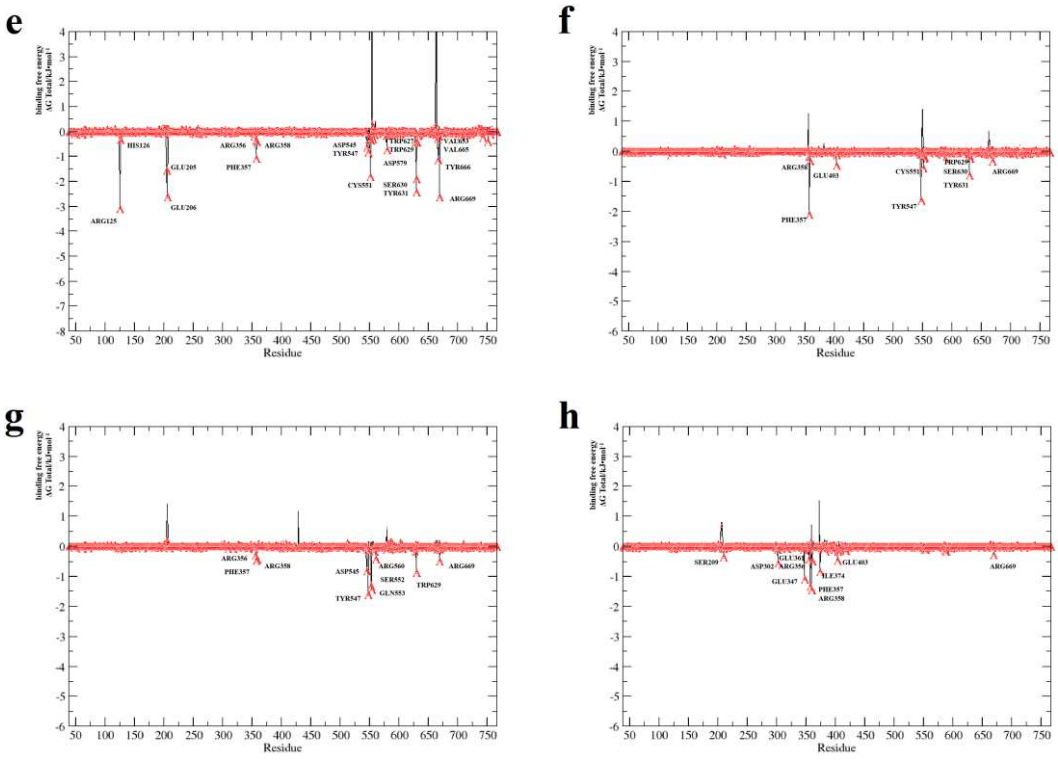

Figure 5. Decomposition free energy results of MOL007103 (a), MOL003714 (b), MOL009665 (c), MOL010404 (d), MOL005400 (e), MOL007062 (f), MOL001965 (g) and MOL003959 (h).

3.3 Comparison of Binding mode

The binding sites of each compounds are summarized in Table 3. The superposition of the eight complexes and DPP-4/Diprotin A (A crystal structure of DPP-4 complex with Diprotin A. PDB ID:1WCY) are shown in Figure 6. It was found that not all inhibitors directly bind to the S_1 or S_2 subsites. MOL010404, MOL001965 and MOL003959 have no obvious interactions with the S_1 or S_2 subsites. However, MOL010404 covers the S_1 subsite or the S_2 subsite by binding the adjacent subsites such as the left S_1', S_2' subsites and the right S_2-extensive subsite stably like a clasp nail and inhibited the activity of DPP-4 efficiently (Figure 6d, Figure 6f). MOL001965 binds to the S_1' and S_2-extensive subsite, MOL003959 binds merely to the S_2-extensive subsite (Figure 6), resulting in the S_1 subsite or S_2 subsite exposed. So MOL001965 and MOL003959 can not prevent the S_1 and S_2 subsites from recognizing the N-terminal and cleaving the dipeptide of GLP-1. Hence, even if MOL001965 and MOL003959 binds to DPP-4 stably, it may not be a effective inhibitor of DPP-4. MOL007103 and MOL009665 could not bind to DPP-4 stably, and deviated from the S_1 and S_2 subsites gradually, so they may also not be effective inhibitors of DPP-4.

Table 3 Occupied subsite analysis of eight compounds with DPP-4

Compound	S_2' subsite	S_1' subsite	S_1 subsite	S_2 subsite	S_2-extensive subsite
MOL007103	+	-	-	-	-
MOL003714	-	+	-	+	-
MOL009665	-	+	-	+	+
MOL010404	+	-	-	-	+
MOL005400	+	+	+	+	-
MOL007062	+	+	+	-	+
MOL001965	-	+	-	-	+
MOL003959	-	-	-	-	+

Note: "+" represents the subsite is occupied

"-" represents the subsite is not occupied

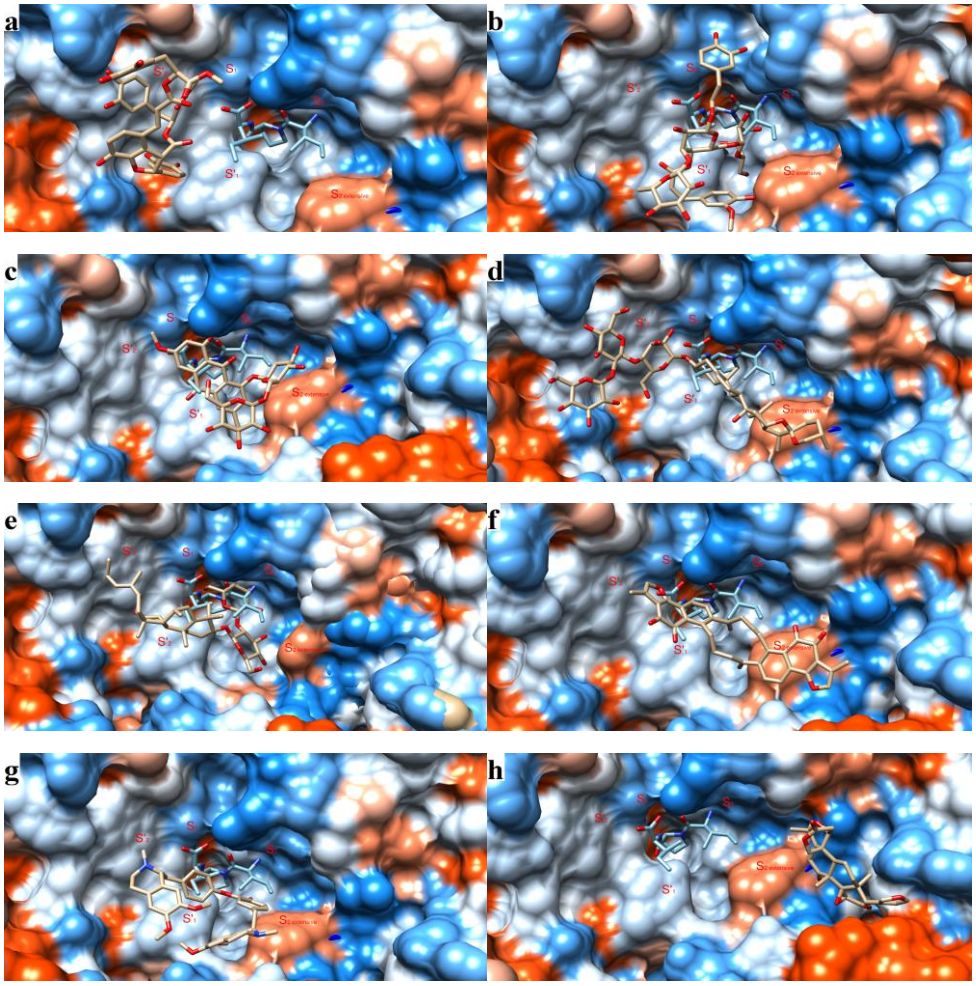

Figure 6 Comparison of Binding modes of MOL007103 (a), MOL003714 (b), MOL009665 (c), MOL010404 (d), MOL005400 (e), MOL007062 (f), MOL001965 (g), MOL003959 (h) and Diprotin A.

(Note: blue sticks represents Diprotin A, brown sticks represents the eight compounds, DPP-4 is represented by hydrophobicity surface, blue and orange surface is the most hydrophilic and the most hydrophobic, respectively)

According to the analysis of binding modes of the eight representative compounds with DPP-4, the possible mechanisms of phenols, steroids and other compounds of Xiao-Ke-An inhibiting DPP-4 are inferred. Firstly, phenolic compounds, MOL003714 have excellent inhibitory effect on DPP-4 as the result of that the hydroxyl groups on the sugar ring form hydrogen bond interactions with residue Glu205, Glu206 and Trp547 and that form van der Waals force with Arg125, Phe357, Trp629 and Tyr631. Secondly, steroids, such as MOL010404 and MOL005400, binding to DPP-4 mainly through glycocycles, also have excellent inhibitory effect on DPP-4. In addition to forming hydrogen bond interactions with Glu205 and Glu206 in the S_2 subsite, the sugar ring of steroids can also form hydrogen bonds with the residues near the S'_2 subsite and form Pi-sigma interaction with Trp629. Thirdly, the compounds of other group contain no polyhydroxy groups in their structures. MOL007062 binds to DPP-4 mainly through Pi-Lone Pair, Pi-Pi and Pi-Alkyl interactions with Tyr547, Trp629 and Phe358 having weaker inhibitory effect on DPP-4 than phenols or steroids.

Besides, MOL001965 is a component that contains nitrogen atoms. Unlike the nitrogen atoms of the drugs mentioned in the introduction forming hydrogen bonds or salt bridges with Arg125, Glu205 and Glu206 in the S_2 subsite, the nitrogen atoms of MOL001965 does not form salt bridge or hydrogen bond with Arg125, Glu205 and Glu206. This could be attributed to that the nitrogen atoms in MOL001965 are tertiary amine nitrogen atoms which are hard to adjust themselves to bind to DPP-4 appropriately and leaves the the key subsites empty; For MOL003959, the compound contains no hydroxyl group merely occupies the S_2-extensive subsite and leaves the the key subsites empty too. So, MOL001965 and MOL003959 may not be the potential DPP-4 inhibitors. Finally, MOL007103 and MOL009665, deviating from the S_1 and S_2 subsites gradually in the process of dynamic simulation, also not be the potential DPP-4 inhibitors.

4. Conclusion

In this study, DPP-4 was used as the target protein, eight representative compounds, MOL003714, MOL001965, MOL010404, MOL007103, MOL009665, MOL005400, MOL003959 and MOL007062 were screened to explore the possible hypoglycemic mechanism of Xiao-Ke-An. It is concluded that (1) The spacious active site of DPP-4 makes it possible that multiple components in Xiao-Ke-An could inhibitor DPP-4 synergistically with different binding modes; (2) The hydrophilic S_2 subsite is a key subsite of DPP-4, so polyhydroxy components prefer to inhibit the activity of DPP-4; (3) MOL003714, which has several phenolic hydroxyl groups and glycocyclic hydroxyl groups and the lowest binding free energy, could be developed into a potent inhibitor for DPP-4. Binding modes of the eight representative compounds of Xiao-Ke-An with DPP-4 theoretically explained hypoglycemic mechanism in molecular level. We expected that Xiao-Ke-An will get more attention in the future.

Authors' contributions Yong-Lin WANG performed the molecular dynamics simulation, the analysis of the results and original draft preparation. Yan ZHUANG contributed to Molecular docking. Chun-Hong DONG, Xiao-Fei LI and Yan TONG reviewed and edited the artical. KONG Yuan-Fang, HU Yu-Long, LI Jie-Ming and WANG Shao-Pei Put forward contributed to the review of the article.

Funding The authors would like to express their gratitude toward the education Department of Henan Province for foundation supports of key research Projects in Henan Province (20A350004).

Data availability N/A

Compliance with ethical standards

Conflict of interest The authors declare that they have no conflict of interest.

Ethics approval N/A

Consent to participate N/A

Consent to publication N/A

Code availability Gaussian 09 package program, Amber2018.

References:

1. Hussain H, Abbas G, Green IR, Ali I (2019) Dipeptidyl peptidase IV inhibitors as a potential target for diabetes: patent review (2015-2018). Expert Opin Ther Pat 29(7):535-553
2. Liakos CI, Papadopoulos DP, Sanidas EA, Markou MI, Hatziagelaki EE, Grassos CA, Velliou ML, Barbetseas JD (2020) Blood Pressure-Lowering Effect of Newer Antihyperglycemic Agents (SGLT-2 Inhibitors, GLP-1 Receptor Agonists, and DPP-4 Inhibitors). Am J Cardiovasc Drugs 262-275
3. Sun ZG, Li ZN, Zhu HL (2020) The Research Progress of DPP-4 Inhibitors. Mini Rev Med Chem 20(17):1709-1718
4. Nong NTP, Chen Y, Shih W, Hsu J (2020) Characterization of Novel Dipeptidyl Peptidase-IV Inhibitory Peptides from Soft-Shelled Turtle Yolk Hydrolysate Using Orthogonal Bioassay-Guided Fractionations Coupled with In Vitro and In Silico Study. Pharmaceuticals 13(10):e308
5. Deacon F C (2020) Dipeptidyl peptidase 4 inhibitors in the treatment of type 2 diabetes mellitus. Nat Rev Endocrinol 16(11):642-653
6. Feng J, Zhang Z, Wallace MB, Stafford JA, Kaldor SW, Kassel DB, Navre M, Shi L, Skene RJ, Asakawa T, Takeuchi K, Xu R, Webb DR, Gwaltney SL (2007) Discovery of Alogliptin: A Potent, Selective, Bioavailable, and Efficacious Inhibitor of Dipeptidyl Peptidase IV. J Med Chem 50(10):2297-2300
7. Liang G, Qian X, Biftu T, Singh S, Gao Y, Scapin G, Patel S, Leiting B, Patel R, Wu J, Zhang X, Thornberry NA, Weber AE (2008) Discovery of new binding elements in DPP-4 inhibition and their applications in novel DPP-4 inhibitor design. Bioorg Med Chem Lett 18(13):3706-3710
8. Nabeno M, Akahoshi F, Kishida H, Miyaguchi I, Tanaka Y, Ishii S, Kadowaki T (2013) A comparative study of the binding modes of recently launched dipeptidyl peptidase IV inhibitors in the active site. Biochem Biophys Res Commun 434(2):191-196
9. Berger JP, SinhaRoy R, Pocai A, Kelly TM, Scapin G, Gao Y, Pryor KAD, Wu JK, Eiermann GJ, Xu SS, Zhang X, Tatosian DA, Weber AE, Thornberry NA, Carr RD (2018) A comparative study of the binding properties, dipeptidyl peptidase-4 (DPP-4) inhibitory activity and glucose-lowering efficacy of the DPP-4 inhibitors alogliptin, linagliptin, saxagliptin, sitagliptin and vildagliptin in mice. Endocrinol Diabetes Metab 1(1):e2
10. Metzler WJ, Yanchunas J, Weigelt C, Kish K, Klei HE, Xie D, Zhang Y, Corbett M, Tamura JK, He B, Hamann LG, Kirby MS, Marcinkeviciene J (2008) Involvement of DPP-IV catalytic residues in enzyme-saxagliptin complex formation. Protein Sci 17(2);240-250
11. Eckhardt M, Langkopf E, Mark M, Tadayyon M, Thomas L, Nar H, Pfrengle W, Guth B, Lotz R, Sieger P, Fuchs H, Himmelsbach F (2007) 8-(3-(R)-Aminopiperidin-1-yl)-7-but-2-ynyl-3-methyl-1-(4-methyl-quinazolin-2-ylmethyl)-3,7-dihydropurine-2,6-dione (BI 1356), a Highly Potent, Selective, Long-Acting, and Orally Bioavailable DPP-4 Inhibitor for the Treatment of Type 2 Diabetes. J Med Chem 50(26):6450-6453
12. Yoshida T, Akahoshi F, Sakashita H, Kitajima H, Nakamura M, Sonda S, Takeuchi M, Tanaka Y, Ueda N, Sekiguchi S, Ishige T, Shima K, Nabeno M, Abe Y, Anabuki J, Soejima A, Yoshida K,

Takashina Y, Ishii S, Kiuchi S, Fukuda S, Tsutsumiuchi R, Kosaka K, Murozono T, Nakamaru Y, Utsumi H, Masutomi N, Kishida H, Miyaguchi I, Hayashi Y (2012) Discovery and preclinical profile of teneligliptin (3-[(2S,4S)-4-[4-(3-methyl-1-phenyl-1H-pyrazol-5-yl)piperazin-1-yl]pyrrolidin-2-ylcarbonyl]thiazolidine): A highly potent, selective, long-lasting and orally active dipeptidyl peptidase IV inhibitor for the treatment of type 2 diabetes. Bioorg Med Chem 20(19):5705-5719

13. Biftu T, Scapin G, Singh S, Feng D, Becker JW, Eiermann G, He H, Lyons K, Patel S, Petrov A, Sinha-Roy R, Zhang B, Wu J, Zhang X, Doss GA, Thornberry NA, Weber AE (2007) Rational design of a novel, potent, and orally bioavailable cyclohexylamine DPP-4 inhibitor by application of molecular modeling and X-ray crystallography of sitagliptin. Bioorg Med Chem Lett 17(12):3384-3387
14. Zhou XJ, Ding L, Liu JX, Su LQ, Dong JJ, Liao L (2019) Efficacy and short-term side effects of sitagliptin, vildagliptin and saxagliptin in Chinese diabetes: a randomized clinical trial. Endocr Connect 8(4):318-325
15. Taylor OM, Lam C (2020) The Effect of Dipeptidyl Peptidase-4 Inhibitors on Macrovascular and Microvascular Complications of Diabetes Mellitus: A Systematic Review. Curr Ther Res Clin Exp 93:100596
16. Kalhotra P, Chittepu V, Osorio-Revilla G, Gallardo-Velázquez T (2018) Structure–Activity Relationship and Molecular Docking of Natural Product Library Reveal Chrysin as a Novel Dipeptidyl Peptidase-4 (DPP-4) Inhibitor: An Integrated In Silico and In Vitro Study. Molecules 23(6):e1368
17. Kalhotra P, Chittepu V, Osorio-Revilla G, Gallardo-Velázquez T (2019) Discovery of Galangin as a Potential DPP-4 Inhibitor That Improves Insulin-Stimulated Skeletal Muscle Glucose Uptake: A Combinational Therapy for Diabetes. Int J Mol Sci 20(5):e1228
18. Akhtar N, Jafri L, Green BD, Kalsoom S, Mirza B (2018) A Multi-Mode Bioactive Agent Isolated From Ficus microcarpa L. Fill. With Therapeutic Potential for Type 2 Diabetes Mellitus. Front Pharmacol 9:e1376
19. Li S, Xu H, Cui S, Zhang Y, Su MB, Gong Y, Qiu S, Jiao Q, Qin C (2016) Discovery and Rational Design of Natural-Product-Derived 2-Phenyl-3,4-dihydro-2H-benzo[f]chromen-3-amine Analogs as Novel and Potent Dipeptidyl Peptidase 4 (DPP-4) Inhibitors for the Treatment of Type 2 Diabetes. J Med Chem 59(14);6772-6790
20. Li S, Qin C, Cui S, Xu H, Wu F, Wang J, Su M, Fang X, Li D, Jiao Q, Zhang M, Xia C, Zhu L, Wang R, Li J, Jiang H, Zhao Z, Li J, Li H (2019) Discovery of a Natural-Product-Derived Preclinical Candidate for Once-Weekly Treatment of Type 2 Diabetes. J Med Chem 62(5):2348-2361
21. Malik LA, Aziz GM, Hiah AHA (2019) The Potential of some Plant Extracts as Radical Scavengers and Dipeptidyl Peptidase-4 Inhibitors. Baghdad Sci J 16(1(Suppl.)):162-168
22. Rios JL, Andujar I, Schinella GR, Francini F (2019) Modulation of Diabetes by Natural Products and Medicinal Plants via Incretins. Planta Med 85(11-12):825-839
23. Yaribeygi H, Atkin SL, Sahebkar A (2019) Natural compounds with DPP‐4 inhibitory effects: Implications for the treatment of diabetes. J Cell Biochem 120(7):10909-10913
24. Kato E (2019) Bioactive compounds in plant materials for the prevention of diabetesand obesity. Biosci Biotechnol Biochem 83(6):975-985
25. Gao Y, Zhang Y, Zhu J (2015) Recent progress in natural products as DPP-4 inhibitors. Future Med Chem 7(8):1079-1089

26. Yang ZZ, Liu W, Zhang F, Li Z, Cheng YY (2015) Deciphering the therapeutic mechanisms of Xiao- Ke-An in treatment of type 2 diabetes in mice by a Fangjiomics approach. Acta Pharmacol Sin 36(6):699-707
27. Jiang S, Wu X, Wang Y, Zou J, Zhao X (2020) The potential DPP-4 inhibitors from Xiao-Ke-An improve the glucolipid metabolism via the activation of AKT/GSK-3beta pathway. Eur J Pharmacol 882:e173272
28. Wu XL, Wang Y, Zhao XP (2016) Screening and identification of DPP-4 inhibitors from Xiaokean formula by a fluorescent probe. Zhongguo Zhong Yao Za Zhi 41(7):1241-1245
29. Ru J, Li P, Wang J, Zhou W, Li B, Huang C, Li P, Guo Z, Tao W, Yang Y, Xu X, Li Y, Wang Y, Yang L. (2014) TCMSP: a database of systems pharmacology for drug discovery from herbal medicines. J Cheminform 6(1):e13
30. Berman H, Henrick K, Nakamura H (2003) Announcing the worldwide Protein Data Bank. Nat Struct Biol 10(12):980
31. M F S (1999) Python: a programming language for software integration and development. J Mol Graph Model 17(1): 57-61
32. Oleg T, Arthur J O (2010) Software News and Update AutoDock Vina: improving the speed and accuracy of docking with a new scoring function, efficient optimization, and multithreading. J Comput Chem 31(2):455-461
33. Salomon-Ferrer R, Götz AW, Poole D, Grand SL, Walker RC (2013) Routine Microsecond Molecular Dynamics Simulations with AMBER on GPUs. 2. Explicit Solvent Particle Mesh Ewald. J Chem Theory Comput 9(9):3878-3888
34. Case DA, Ben-Shalom IY, Brozell SR, Cerutti DS, Cheatham III TE, Cruzeiro VWD, Darden TA, Duke RE, Ghoreishi D, Gilson MK, Gohlke H, Goetz AW, Greene D, Harris R, Homeyer N, Huang Y, Izadi S, Kovalenko A, Kurtzman T, Lee TS, LeGrand S, Li P, Lin C, Liu J, Luchko T, Luo R, Mermelstein DJ, Merz KM, Miao Y, Monard G,; Nguyen C, Nguyen H, Omelyan I, Onufriev A, Pan F, Qi R, Roe DR, Roitberg A, Sagui C, Schott-Verdugo S, Shen J, Simmerling CL, SmithvJ, Salomon-Ferrer R, Swails J, Walker RC, Wang J, Wei H, Wolf RM, Wu X, Xiao L, York DM and Kollman PA (2018) AMBER 2018, University of California, San Francisco
35. Frisch MJ, Trucks G, Schlegel HB, Scuseria GE, Robb MA, Cheeseman JR, Scalmani G, Barone V, Mennucci B, Petersson G. A, Nakatsuji H, Caricato M, Li X,Hratchian HP, Izmaylov AF, Bloino J, Zheng G, Sonnenberg JL, Hada M, Ehara M, Toyota K, Fukuda R, Hasegawa J, Ishida M, Nakajima T, Honda Y, Kitao O, Nakai H,Vreven T, Montgomery JAJr, Peralta JE, Ogliaro F, Bearpark M, Heyd JJ, Brothers E, Kudin KN, Staroverov VN, Keith T, Kobayashi R, Normand J, Raghavachari K, Rendell A, Burant JC, Iyengar SS, Tomasi J, Cossi M, Rega N, Millam JM, Klene M, Knox JE, Cross JB, Bakken V, Adamo C, Jaramillo J, Gomperts R, Stratmann RE, Yazyev O, Austin AJ, Cammi R, Pomelli C, Ochterski JW, Martin RL, Morokuma K, Zakrzewski VG, Voth GA, Salvador P, Dannenberg JJ, Dapprich S, Daniels AD, Farkas O, Foresman JB, Ortiz JV, Cioslowski J, Fox DJ (2010) GAUSSIAN 09 (revision C.01) Inc., Wallingford CT
36. Maier JA, Martinez C, Kasavajhala K, Wickstrom L, Hauser KE, Simmerling C (2015) ff14SB: Improving the Accuracy of Protein Side Chain and Backbone Parameters from ff99SB. J Chem Theory Comput 11(8):3696-3713
37. Miller BR, McGee TD, Swails JM, Homeyer N, Gohlke H, Roitberg AE (2012) MMPBSA.py: An Efficient Program for End-State Free Energy Calculations. J Chem Theory Comput 8(9):3314-3321

38. El-Barghouthi M I, Jaime C, Al-Sakhen NA, Issa AA, Abdoh AA, OmariMMA, Badwan AA, Zughul MB (2008) Molecular dynamics simulations and MM-PBSA calculations of the cyclodextrin inclusion complexes with 1-alkanols, para-substituted phenols and substituted imidazoles. J Mol Struct-Theochem 853(1-3):45-52
39. Wang JM, Hou TJ, Xu XJ (2006) Recent Advances in Free Energy Calculations with a Combination of Molecular Mechanics and Continuum Models. Curr Comput-Aid Drug 2(3):287-306

Figures

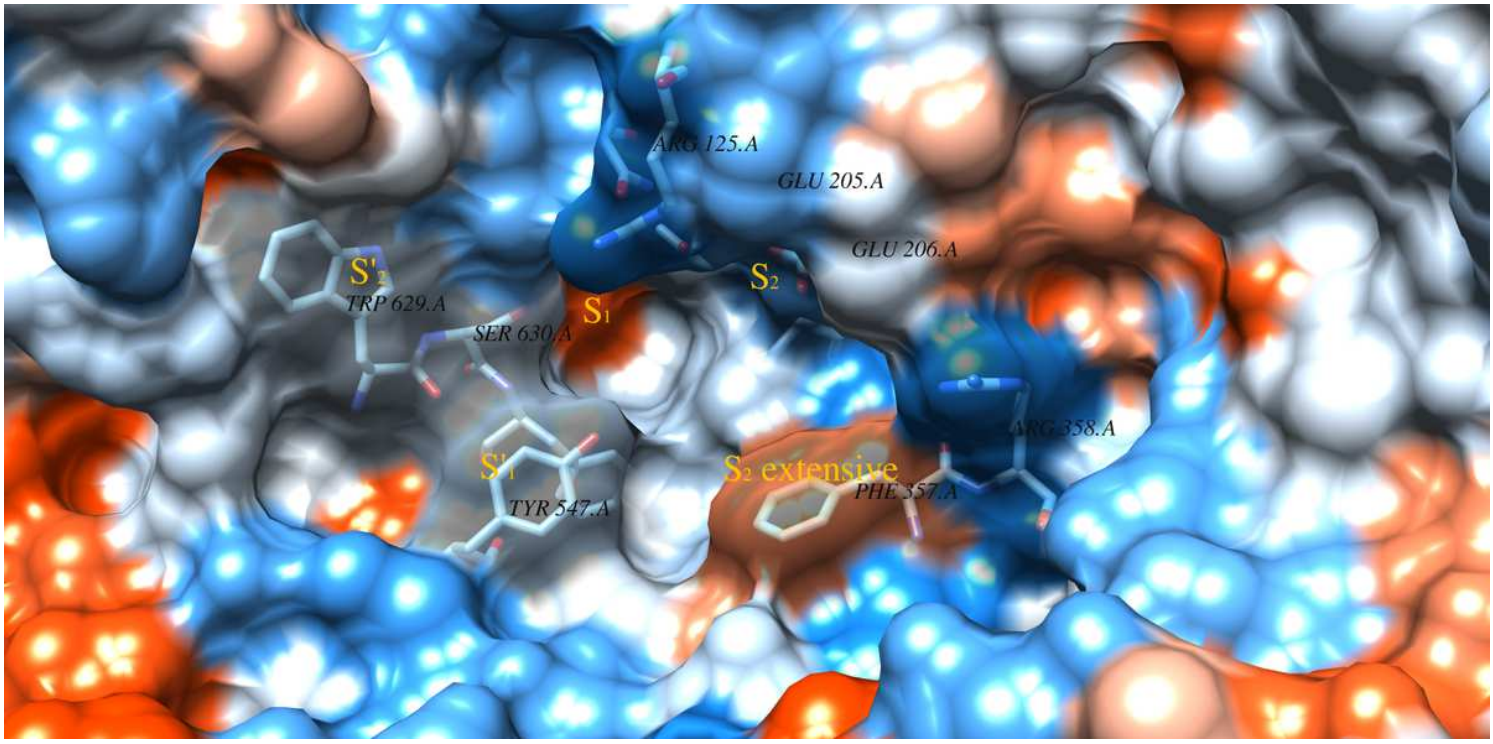

Figure 1

The distribution of each subsite of DPP-4

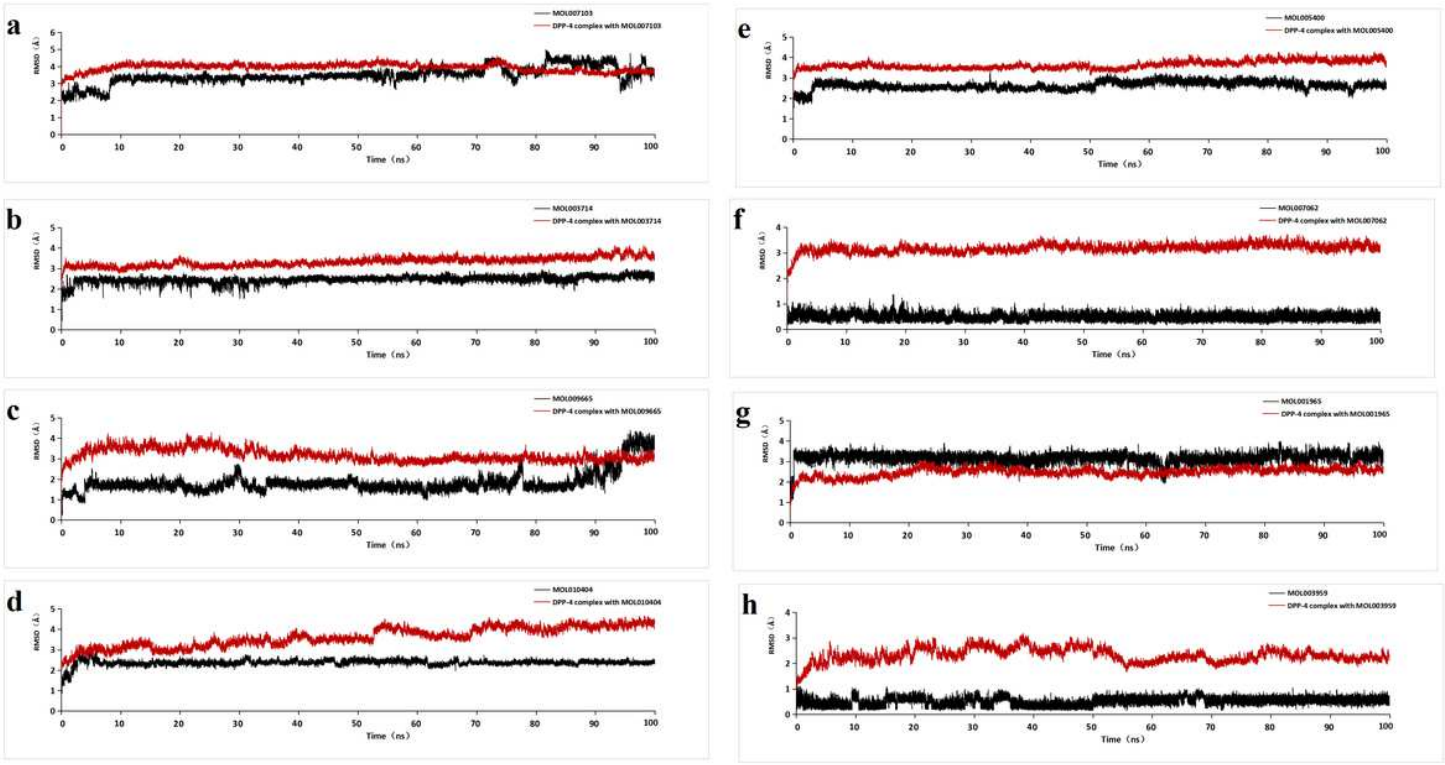

Figure 2

RMSD plots of DPP-4 in complex with MOL007103 (a), MOL003714 (b), MOL009665 (c), MOL010404 (d), MOL005400 (e), MOL007062 (f), MOL001965 (g) and MOL003959 (h).

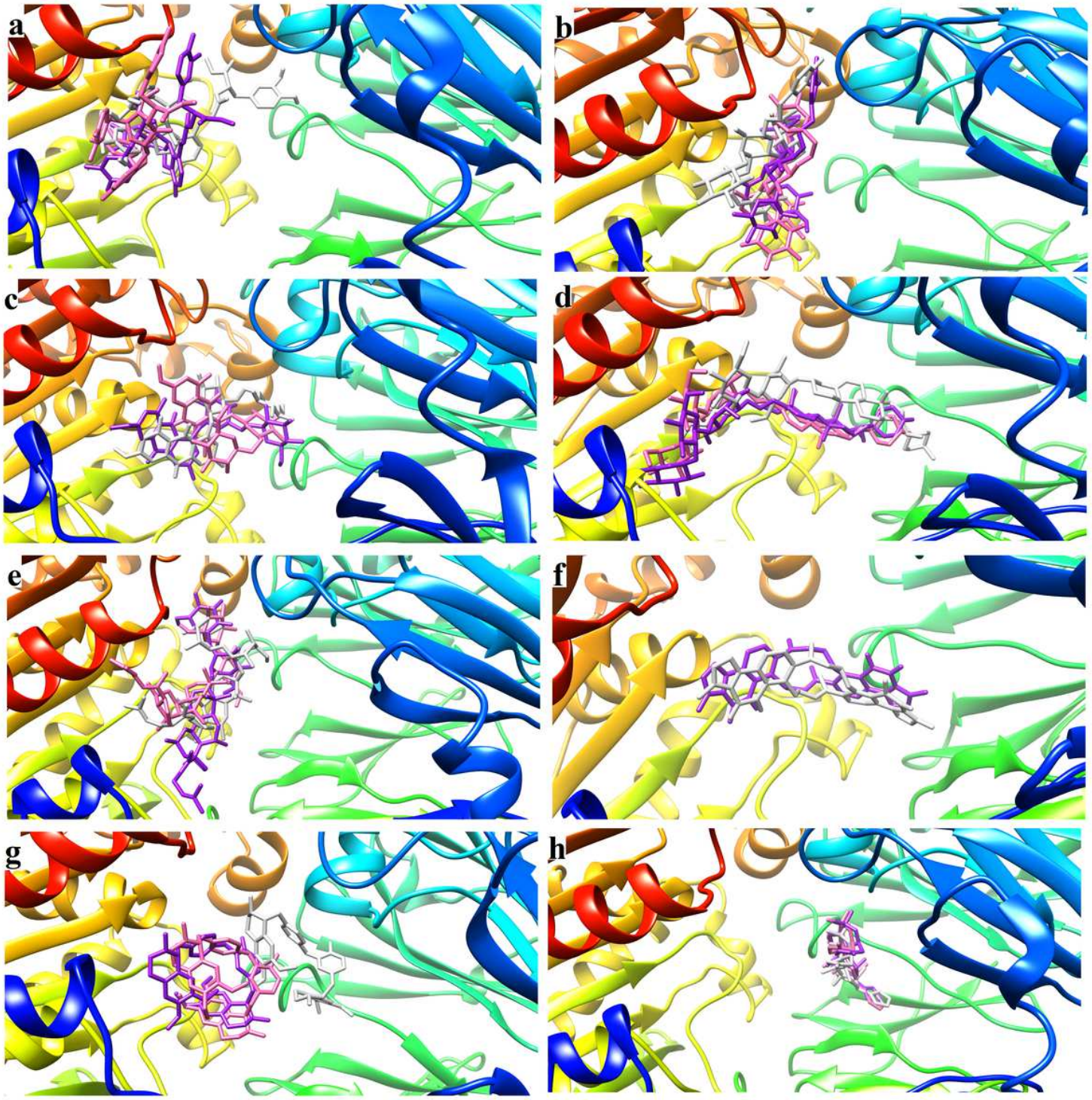

Figure 3

Superposition of the eight compounds in the dynamics simulation process. The ribbon model represents DPP-4. The stick model represents the eight compounds, gray stick represents the initial conformation. In (a), purple and pink sticks represent the conformations of MOL007103 at 50 ns and 100 ns, respectively; In (b), purple and pink sticks represent the conformations of MOL003714 at 10 ns and 100 ns,

respectively; In (c), purple and pink sticks represent the conformations of MOL009665 at 50 and 100 ns, respectively; In (d), purple and pink sticks represent the conformations of MOL010404 at 10 ns and 100 ns, respectively; In (e), purple and pink sticks represent the conformations of MOL005400 at 5 ns and 100 ns, respectively; In (f), pink sticks represent the conformation of MOL007062 at 100 ns; In (g), purple and pink sticks represent the conformations of MOL001965 at 2 ns and 100 ns, respectively; In (h), purple, pink and orange sticks represent the conformations of MOL003959 at 50 ns and 100 ns, respectively.

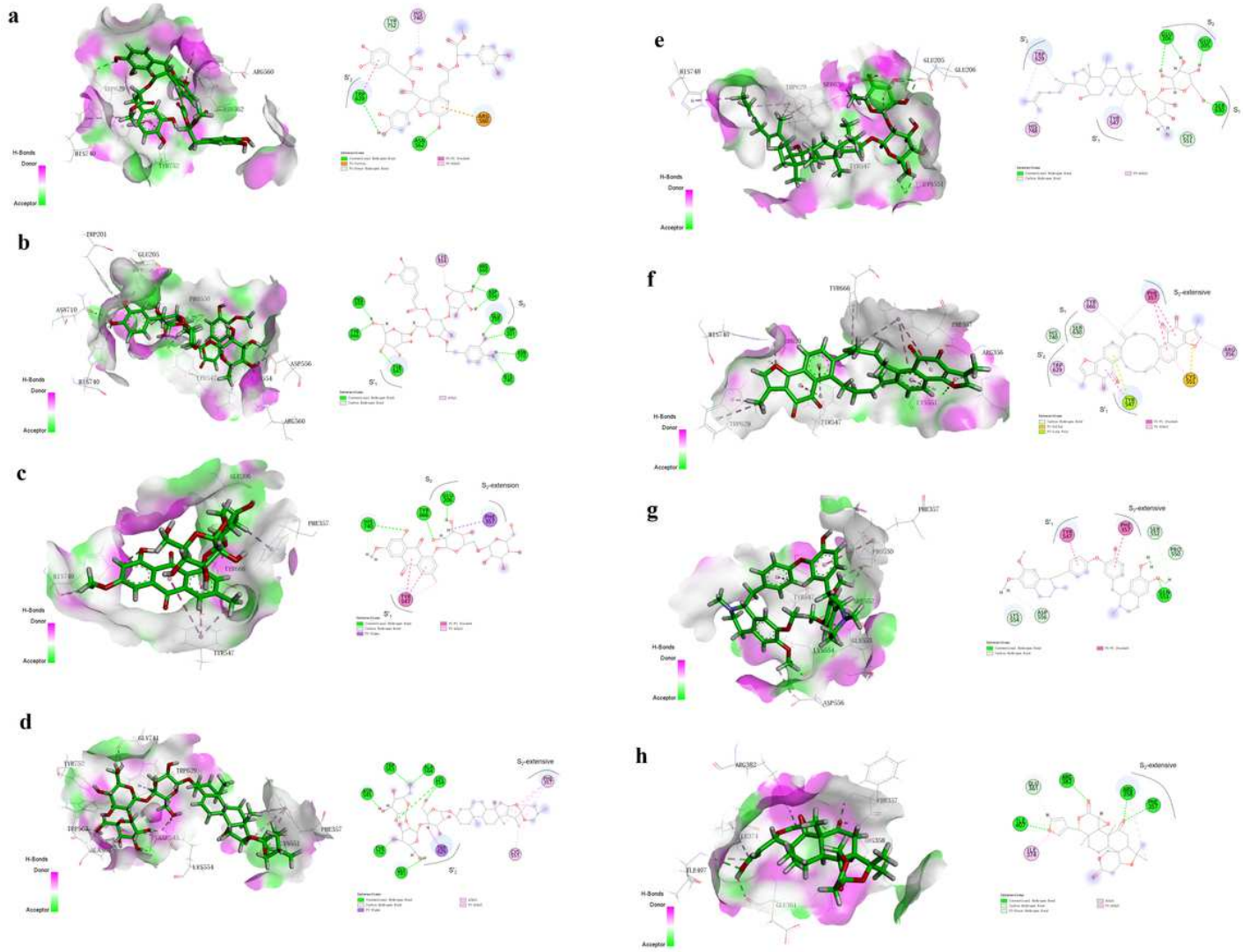

Figure 4

Binding modes and interaction diagrams of MOL007103 (a), MOL003714 (b), MOL009665 (c), MOL010404 (d), MOL005400 (e), MOL007062 (f), MOL001965 (g) and MOL003959 (h) with DPP-4.

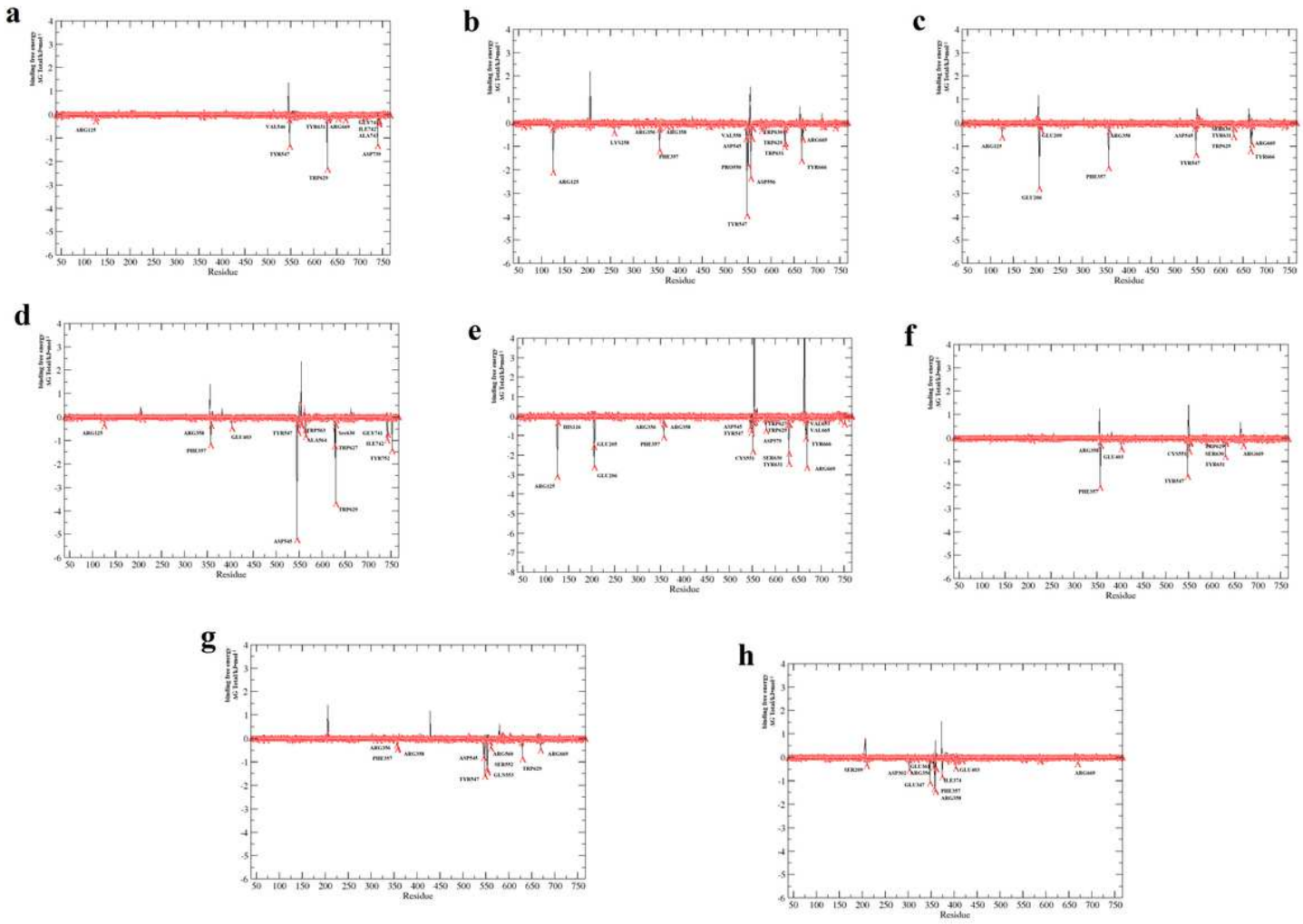

Figure 5

Decomposition free energy results of MOL007103 (a), MOL003714 (b), MOL009665 (c), MOL010404 (d), MOL005400 (e), MOL007062 (f), MOL001965 (g) and MOL003959 (h).

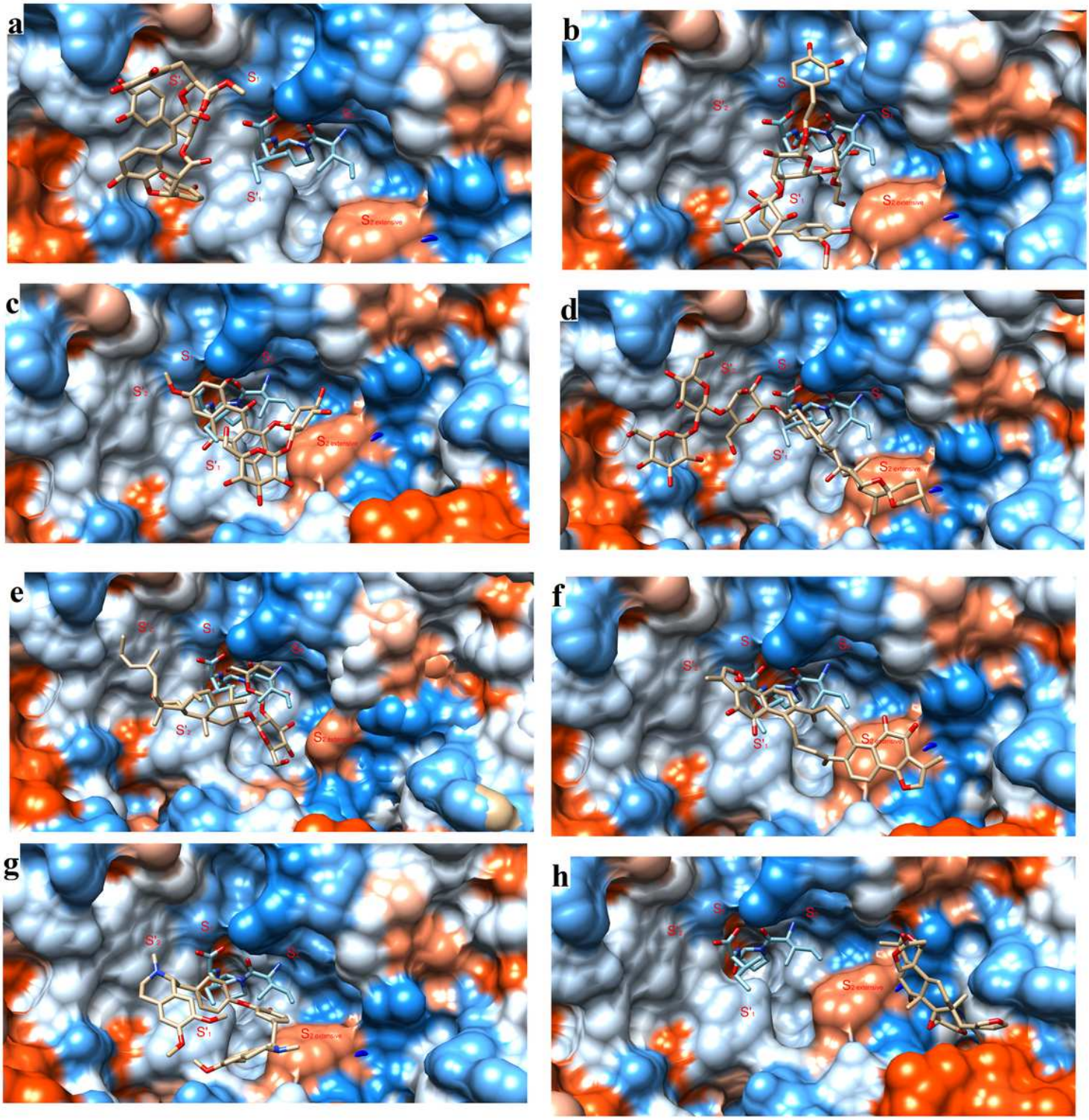

Figure 6

Comparison of Binding modes of MOL007103 (a), MOL003714 (b), MOL009665 (c), MOL010404 (d), MOL005400 (e), MOL007062 (f), MOL001965 (g), MOL003959 (h) and Diprotin A. (Note: blue sticks represents Diprotin A, brown sticks represents the eight compounds, DPP-4 is represented by hydrophobicity surface, blue and orange surface is the most hydrophilic and the most hydrophobic, respectively)